

# Effect of post-growth annealing on the optical properties of LiGaS<sub>2</sub> nonlinear crystals

Alexander Yelissejev<sup>a)</sup>, Marina Starikova<sup>b)</sup>, Ludmila Isaenko<sup>a)</sup>,  
Sergei Lobanov<sup>a)</sup>, Valentin Petrov<sup>c)</sup>

<sup>a)</sup>Institute of Geology and Mineralogy, SB RAS, 43 Russkaya Str., 630058 Novosibirsk, Russia;

<sup>b)</sup>Novosibirsk State Technical University, 20 K. Marx Ave., 630028 Novosibirsk, Russia;

<sup>c)</sup>Max-Born-Institute for Nonlinear Optics and Ultrafast Spectroscopy, 2A Max-Born-Str.,  
D-12489 Berlin, Germany

## ABSTRACT

High chalcogen volatility and Li interaction with the container walls result in variation of crystal composition and presence of both extended and point defects in as-grown LiGaS<sub>2</sub> nonlinear crystals. Annealing in appropriate conditions is used to correct the composition and improve the optical quality. We annealed LiGaS<sub>2</sub> in vacuum, in the presence of Li<sub>2</sub>S, Ga<sub>2</sub>S<sub>3</sub>, and S, and studied changes in transmission, photoluminescence and photo-induced absorption. OH groups, S-H and S-S complexes, sulfur vacancies and cation antisite defects (Ga<sub>Li</sub>) are most important. Photo-induced absorption is reversible: It appears after illumination with UV/blue light and disappears after illumination with IR light or by heating the sample.

Key words: nonlinear optical crystals; annealing; defects; optical properties

## 1. INTRODUCTION

Practical solid-state-lasers generate wavelengths up to  $\sim 3 \mu\text{m}$ , with the most prominent representatives in this limit being the fixed wavelength Er<sup>3+</sup>-lasers and the tunable Cr<sup>2+</sup>-lasers.<sup>1</sup> The spectral range above  $3 \mu\text{m}$  in the mid-IR can be continuously covered by nonlinear frequency down-conversion using powerful laser sources in the near-IR. Oxide-based nonlinear crystals can be pumped by widely-spread high-power diode-pumped laser systems, such as Nd:YAG, and perform well up to about  $4 \mu\text{m}$ , but their performance at longer wavelengths is dramatically affected by the onset of multi-phonon mid-IR absorption. Since nonlinear frequency conversion is intensity dependent process, high efficiency can be expected only using pulsed laser sources (femtosecond to nanosecond). At practical pump intensities, most of the chalcogenide (non-oxide) mid-IR nonlinear crystals will suffer two-photon absorption (TPA) at the pump wavelength of 1064 nm because of their low band-gap. This is a serious constraint with regard to picosecond or nanosecond down-conversion devices for the mid-IR (optical parametric generators, amplifiers and oscillators) because only few nonlinear crystals transparent in the mid-IR exhibit a band-gap corresponding to wavelengths shorter than say 532 nm.<sup>2</sup> The situation is even more critical in the femtosecond regime where one normally starts from the 800 nm band of Ti:sapphire lasers/amplifiers employed as pump sources. Thus, the lithium ternary chalcogenides with the chemical formula LiBC<sub>2</sub> where B=In and Ga, C=S, Se or Te, occupy a special position among the non-oxide nonlinear crystals because they are characterized by the widest band-gaps.<sup>3,4</sup> As a consequence, these compounds exhibit increased damage threshold and relatively low refractive index dispersion in the infrared which is important for frequency conversion of short laser pulses. In addition, their thermal conductivity is higher than for their Ag analogues, which is an essential advantage at high average powers. However, it should be emphasized that the practical application of these crystals is to a great extent dependent on the level of perfection of their growth technology and the achievable optical quality. Unfortunately, the growth of such crystals is rather complex and deviation from stoichiometry is typical for the chalcogenides of the LiBC<sub>2</sub> family because of the high chemical activity of lithium and the sulfur volatility. Post-growth annealing in appropriate

atmosphere is usually used to achieve the desired crystal composition and get closer to the stoichiometric formula.

Though exhibiting relatively low nonlinear coefficients,  $\text{LiGaS}_2$  (LGS) possesses the widest band-gap among the  $\text{LiBC}_2$  compounds<sup>3</sup> and recently we established that it is also the compound characterized by highest damage threshold at 1064 nm (using nanosecond pulses) and by no aging (no surface deterioration after periods of more than 5 years). Its lowest dispersion and its resistivity against gray track formation were indeed advantageous in optical parametric down-conversion experiments with femtosecond pump pulses near 800 nm.<sup>5</sup> At the same time information on structural defects in this compound and their influence on the spectroscopic features is scarce. The present work tries to fill this gap by studying the effect of the post-growth treatment conditions on the optical properties of nonlinear LGS crystals.

## 2. CRYSTAL GROWTH AND SPECTROSCOPY

The LGS single crystals were grown using the Bridgman-Stockbarger technique, in a double-zone vertical furnace. The upper and lower zones were separated by a diaphragm from heat-insulating material. The temperature of the melting zone was maintained at about 1150°C (roughly 100°C above the melting temperature) with an accuracy of  $\pm 0.1^\circ\text{C}$ . The axial temperature gradient was  $\sim 2^\circ/\text{mm}$ . Typical rates for the ampoule sinking were 2 to 10 mm/day. The starting reagents were with 99.999% (Ga, S) and 99.9% (Li) purity. The charge was placed into a glass-graphite crucible and the latter was located in a silica ampoule. Such construction allows one to avoid the chemical reaction between lithium and the walls of the silica ampoule. The obtained LGS crystals were  $\sim 20$  mm in diameter and  $\sim 50$  mm in length. From the same as-grown boule we prepared 5 oriented (001) plates, with thickness  $L \sim 1.75$  mm and apertures of  $\sim 0.5$  cm<sup>2</sup>, Fig. 1. These plates were then annealed at  $\sim 950^\circ\text{C}$  for two days in different atmospheres: in vacuum and in the presence of solid  $\text{Li}_2\text{S}$ ,  $\text{Ga}_2\text{S}_3$ , and S, in order to improve the transparency, Fig. 2. From our previous data on the composition of the related  $\text{LiInS}_2$ , obtained using the differential dissolution technique,<sup>6</sup> compositional changes of  $\sim 2$  to 3 wt. % for different components could be expected as a result of the annealing. The annealed LGS plates were polished for the spectroscopic studies.



Fig. 1. LGS samples before (1) and after annealing in vacuum (2),  $\text{Li}_2\text{S}$  (3),  $\text{Ga}_2\text{S}_3$  (4) and S (5).

The transmission spectra were measured using a conventional spectrophotometer in the UV to near-IR spectral range and a Fourier-transform spectrophotometer in the mid-IR. Photoluminescence (PL) spectra were obtained with an SDL1 spectrometer after excitation with a 1 kW Xe lamp through a MDR2 monochromator. The crystal under investigation was placed in a metal vacuum cryostat and its temperature was varied in the range from 80 to 700 K.

## 3. TRANSMISSION SPECTRA

The transmission spectra for LGS crystals, both as grown and annealed in different atmospheres, are shown in Fig. 2. At room temperature, LGS is transparent in the 0.33-11.7  $\mu\text{m}$  range at the transmission level of 10%. The short wave limit

in the UV is determined by the fundamental absorption edge of LGS whereas multi-phonon absorption is responsible for the long wave limit: two-phonon and three-phonon absorption limits setting on from about 10 and 7  $\mu\text{m}$ , respectively. The band gap value, estimated with thin ( $\sim 100 \mu\text{m}$ ) LGS plates, is 4.15 eV at room temperature.<sup>7</sup>

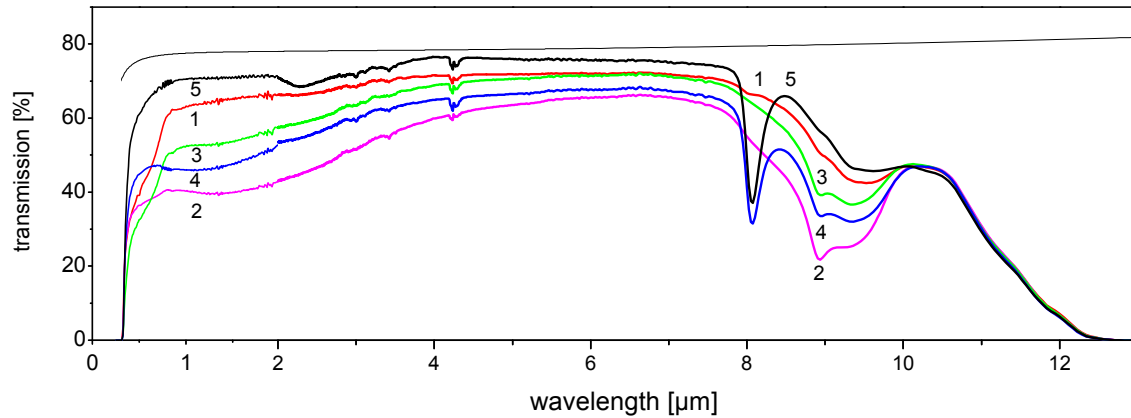


Fig. 2. Transmission spectra of LGS recorded at 300 K in the transparency region from UV to mid-IR: before (1) and after annealing in vacuum (2),  $\text{Li}_2\text{S}$  (3),  $\text{Ga}_2\text{S}_3$  (4) and S (5). The thin line shows the maximum possible transmission of LGS in the case of no absorption, taking into account multiple reflections for the uncoated samples.

In comparison to other crystals of the  $\text{LiBC}_2$  family, the as-grown LGS crystals exhibit relatively low light scattering on small inclusions of foreign phases. For other ternary chalcogenides, including  $\text{AgGaS}_2$ ,  $\text{AgGaSe}_2$ , and  $\text{LiInS}_2$ , as-grown crystals are milky,<sup>4,7</sup> and to improve their transparency it is necessary to anneal them in appropriate atmosphere. The as-grown LGS crystals have a relatively good transparency of up to 70% in the mid-IR whereas the theoretical limit is  $\sim 78\%$  at 5  $\mu\text{m}$  (see Fig. 2). The reduced transparency at wavelengths below 4  $\mu\text{m}$  in the spectra (2)-(4) is associated with the combined effect of absorption of point and extended defects, and light scattering on small submicron inclusions of foreign phases. Extended defects such as dislocations are known to produce a continuous set of levels in the forbidden zone which results in an unstructured absorption at short wavelengths.<sup>8</sup> Light scattering efficiency is inversely proportional to the wavelength ( $\sim \lambda^{-4}$ ) and the corresponding losses increase at shorter wavelengths. Consequently, the actual transparency is higher at longer wavelengths (Fig. 2). All LGS crystals are colorless but they look slightly grayish after annealing in vacuum,  $\text{Li}_2\text{S}$  and  $\text{Ga}_2\text{S}_3$ . A rose tint is seen in as-grown samples and such annealed in  $\text{Li}_2\text{S}$  (Fig. 1).

From Fig. 2, it is possible to compare the transmission spectra of the LGS plates after annealing in different conditions (in vacuum, in the presence of solid  $\text{Li}_2\text{S}$ ,  $\text{Ga}_2\text{S}_3$ , and S). All spectra exhibit weak absorption features at 3.0, 3.4 and 4.3  $\mu\text{m}$  (Fig. 1). The first two features can be related to OH groups whereas the feature near 4.3  $\mu\text{m}$  may be associated with S-H vibrations with H in Li site or as an interstitial H.<sup>9</sup> All these features can be attributed to the presence of moisture in the starting materials: commercially available sulfur and sulfur compounds (such as  $\text{Li}_2\text{S}$  and  $\text{Ga}_2\text{S}_3$ ) are often contaminated with moisture since they are usually precipitated from aqueous solutions. Similar peaks are found also in  $\text{As}_2\text{S}_3$  glass.<sup>9</sup> Annealing in  $\text{Ga}_2\text{S}_3$  and S produces strong absorption near 8  $\mu\text{m}$  which is due to S-S bonds.<sup>9</sup> In this case S should occupy a metal site (presumably a Li site). The bands at 8.9 and 9.3  $\mu\text{m}$  appear after annealing in vacuum,  $\text{Li}_2\text{S}$  and  $\text{Ga}_2\text{S}_3$  (Fig. 2). Numerous metal-oxygen bonds absorb in this spectral range as well, hence, oxygen impurities (in the sulfur site) are one probable source for this absorption, in particular taking into account that  $\text{H}_2\text{O}$  is such a common contaminant as outlined above. Our experience with  $\text{LiInS}_2$ ,<sup>6</sup> indicates that the annealing procedures employed modify the content of some components in the crystal volume but may also result in inclusions of foreign phases. The work on optimization of the annealing procedure is in progress: The goal is to correct the composition and to increase the transparency without any additional absorption in inclusions.

Fragments of the transmission spectra in the region near the fundamental absorption edge are shown in Fig. 3. For easier comparison of the shapes, the transmission is adjusted to 100% at 450 nm for all spectra. One can see that as-grown LGS exhibits the shortest UV limit in the transparency. All types of annealing shift this edge to longer wavelengths: The shift

amounts to 1.5, 4, 6 and 12 nm for annealing in Li<sub>2</sub>S, vacuum, Ga<sub>2</sub>S<sub>3</sub> and S, respectively. Analysis of the absorption edge shape gives straight lines in coordinates  $\ln(\alpha L) = f(h\nu)$ , which corresponds to the well-known Urbach's rule:  $\alpha \sim \exp[-(E_g - h\nu)/kT]$ .<sup>10</sup> The reasons for such a behavior are related to accidental inhomogeneities in electric fields and stresses in the crystal structure, which in turn lead to "tails" of states/absorption.

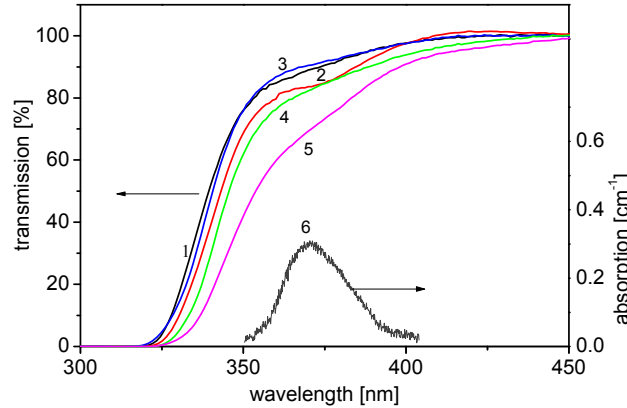


Fig. 3. Comparison of the shape of the fundamental absorption edge of LGS at 300 K before (1) and after annealing in vacuum (2), Li<sub>2</sub>S (3), Ga<sub>2</sub>S<sub>3</sub> (4) and S (5). All spectra are normalized to 100% transmission at 450 nm. Curve (6) shows the weak absorption band centered near 370 nm which affects the shape of spectra (2) and (5).

The transparency edge is located near 320 nm at 300 K and shifts to 310 nm at 80 K. It is interesting that the band at 330 nm,<sup>7</sup> with an intensity of  $\sim 20 \text{ cm}^{-1}$ , is not seen in Fig. 3. The only feature in this region is a weak band near 370 nm. This band is most pronounced in the sample annealed in vacuum, curve (2) in Fig. 3, and it seems to be present also in LGS annealed in the presence of sulfur, curve (5). Curve (6) in Fig. 3 is obtained as a differential absorption spectrum by subtracting the spectrum for case (1) from that for case (2). It can be seen that the intensity of the 370 nm band is  $\sim 0.3 \text{ cm}^{-1}$  and that it is asymmetric, with half widths at half maximum (HWHM) of 9 and 15 nm, respectively.

#### 4. PHOTOLUMINESCENCE SPECTRA

UV light from 250 to 340 nm excites intense yellow-red PL in all LGS crystals. This PL corresponds to a broad band centered near 650 nm, with a HWHM  $\sim 80 \text{ nm}$ , Fig. 4, curves (1) and (3). The position of its maximum varies slightly depending on excitation wavelength, crystal temperature and type of annealing. In as-grown LGS we found also a weak violet PL which can be excited near 370 nm: Its spectrum consists of a main band at 426 nm with a HWHM of 16 nm and a satellite at 510 nm (HWHM = 20 nm), see curve (4) in Fig. 4. The following changes are observed in the PL spectra of LGS crystals after annealing:

- (i) After annealing in vacuum, intense blue PL with the most intense band at 450 nm and a satellite at  $\sim 533 \text{ nm}$  appears, curve (2) in Fig. 4. The HWHM values for these two bands are 17 and 20 nm, respectively;
- (ii) After annealing in Li<sub>2</sub>S and Ga<sub>2</sub>S<sub>3</sub>, the blue PL is considerably quenched whereas a weak band near 900 nm, with a HWHM of  $\sim 50 \text{ nm}$ , appears;
- (iii) After annealing in sulfur, violet ( $\sim 426 \text{ nm}$ ) PL becomes the most intense, with a satellite at  $\sim 510 \text{ nm}$ , curve (4) in Fig. 4.

The large width of the PL bands ( $>30 \text{ nm}$ ) and the absence of fine structure even at low temperature (4.2 K) suggest a strong electron-phonon interaction in LGS as in the case of other crystals of the LiBC<sub>2</sub> family. The shape of the bands is close to Gaussian in this case. We also found strong temperature quenching: the PL intensity decreases by an order of magnitude as the temperature is increased from 80 to 300 K.

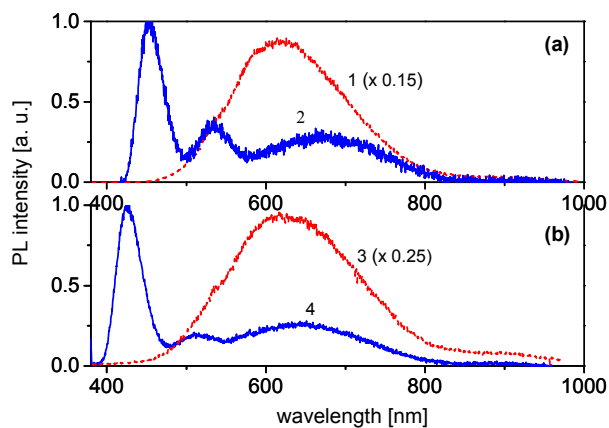


Fig. 4. PL spectra for LGS recorded at 80 K, after annealing in vacuum (a) and in sulfur (b). The excitation wavelength was 300 nm for curves (1, 3) and 375 nm for curves (2, 4).

## 5. PHOTOEXCITATION SPECTRA

If the emission wavelength is fixed when measuring PL and the excitation wavelength is scanned, one obtains the photoluminescence excitation (PLE) spectrum, after correction for the spectral distribution of the Xe lamp source. Such spectroscopy gives information about the absorption spectrum of the luminescence center even when its contribution to the absorption spectrum recorded in the usual way is very weak. Figure 5 shows PLE spectra for the main PL emissions in LGS.

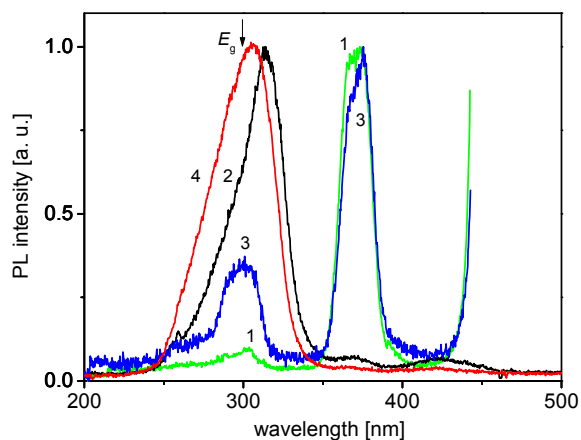


Fig. 5. PLE spectra of LGS recorded at 80 K. The samples measured were annealed in vacuum, curves (1, 2), and in sulfur, curves (3, 4). The emission was recorded at 450 nm (1), 650 nm (2, 4) and 426 nm (3). All spectra are normalized to the maximum of the main band. The arrow shows the band-gap (4.15 eV) determined from absorption measurements.

Curves (1) and (3) in Fig. 5 show PLE spectra for blue and violet PL in the 450 and 426 nm emission bands, for samples annealed in vacuum and sulfur, respectively. Curves (2) and (4) correspond to PL in the 650 nm band from the same two samples. One can see that these PLE spectra are similar in the 350 to 380 nm range and agree well with the 370 nm

absorption band in Fig. 3. Most likely there is a doublet in this spectral range. After annealing in sulfur there is no Stokes shift and the zero-phonon line should be at about 400 nm. After annealing in vacuum, the PL band is shifted to longer wavelengths (450 nm) and the Stokes shift is  $\sim 0.15$  eV. Another band at  $\sim 300$  nm is related to band-to-band transitions and it agrees well with the  $E_g=4.15$  eV band-gap value (see arrow position in Fig. 5), determined from absorption spectroscopy.<sup>6</sup> The 300 nm band is weak in comparison to the 450/426 nm bands which means that intracenter excitation is much more effective to produce blue PL than band-to-band excitation. It is obvious that anion vacancies  $V_S$  are the main defects produced under vacuum annealing which is a result of the high sulfur volatility. Such defects might be present in as-grown LGS crystals and their concentration will increase after vacuum annealing but decrease after annealing in the presence of  $Li_2S$ ,  $Ga_2S_3$  and S. Such scenario agrees with the behavior of the blue 450 nm PL and thus this PL can be related to  $V_S$  vacancies.

The surprising similarity of the PL band pairs at 450/533 nm and 426/510 nm (similar doublet structure in PL and identical spectra in absorption/PLE) suggests that we deal with defects similar in structure, presumably different vacancies  $V_S$ . Typically, annealing in sulfur produces some surplus interstitial sulfur ( $S_i$ ), which annihilates further with vacancies  $V_S$  and the contribution from  $V_S$  should become weaker. The PL in the 426/510 nm bands after annealing in sulfur may be explained by the fact that there are  $V_S$  vacancies of different stability depending on their position in the lattice and only some of them annihilate.

The PL emission at 650 nm, present for all examined LGS samples, is excited by band-to-band transitions as well as, with much higher efficiency, through the near-edge band at 330 nm. This band has been observed in Ref. 7 in absorption spectra but as already mentioned it is very weak in the present LGS crystals. This yellow to red emission is likely due to an antisite defect which is typical for multicomponent chalcogenide compounds. Taking into account that the cavities in the LGS lattice are occupied by  $Li^+$  and  $Ga^{3+}$  cations with radii of 0.045 and 0.042 nm, respectively,<sup>11</sup> this could be  $Ga^{3+}$  in Li position but not vice versa. An alternative explanation of the 650 nm PL band could be the recombination of donor-acceptor pairs, by analogy with other  $A^I B^{III} C_2^{VI}$  compounds.<sup>12</sup> The pair components could be lithium as donor and gallium vacancy as acceptor.

## 6. PHOTO-INDUCED ABSORPTION

Since nonlinear crystals such as LGS are intended for use in strong light fields, at high intensity of the pump radiation, we studied also the changes in the LGS absorption after illumination. Figure 6 shows the absorption spectrum from the UV to the near-IR for as-grown LGS before, curve (1), and after, curve (2), focused illumination with a 100 W Hg lamp through an UFS1 cut-off glass filter which transmits in the 270 to 400 nm range.

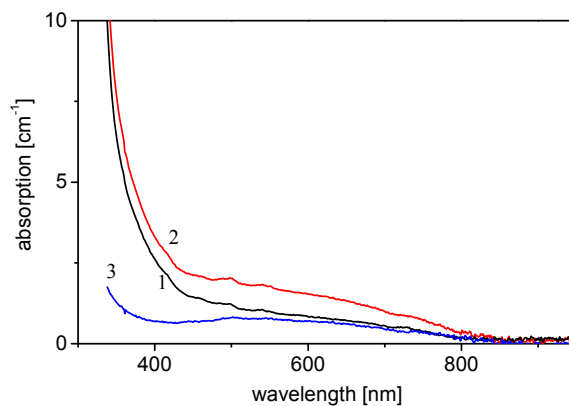


Fig. 6. LGS absorption spectra recorded at 300 K before (1) and after illumination during 10 minutes with the UV light from a Hg lamp (through an UFS1 glass filter) (2). Curve (3) is a differential spectrum (3=2-1).

One can see that UV illumination leads to an increase by  $\sim 1 \text{ cm}^{-1}$  in the absorption at wavelengths below 850 nm. Visual examination shows that there is local darkening in the LGS plate in the place of illumination. This photoinduced absorption (PIA) effect was found to be reversible: The initial transparency could be restored after illumination of the samples with light above 600 nm or after heating it to 400°C. Such behavior of the PIA under illumination with light of different wavelengths and heating is typical for crystals with defects which have levels close to the valence or conduction bands in the energy diagram. Such defects are capture centers for charge carriers. PIA has been observed earlier in other nonlinear crystals such as lithium and potassium niobates<sup>13</sup> as well as in  $\text{LiInS}_2$ ,<sup>4</sup> where PIA is responsible for the well-known gray tracks. PIA is considered to depend on the set and concentration of the existing point defects and affects to a great extent the performance of the nonlinear crystals in high power frequency conversion schemes.

## 7. CONCLUSION

As grown LGS crystals were found to contain much lower concentration of foreign phase inclusions in comparison to the other compounds belonging to the  $\text{LiBC}_2$  family of wide band-gap mid-IR nonlinear crystals with B=In and Ga, C=S, Se or Te. Changes after annealing in different atmosphere (in vacuum, in the presence of solid  $\text{Li}_2\text{S}$ ,  $\text{Ga}_2\text{S}_3$  or S) were analyzed in the LGS transmission spectra. A broad yellow-red PL band was observed at short-wave excitation (due to band-to-band transitions as well as to the 330 nm near-edge band): It is related to cation antisite defects  $\text{Ga}_{\text{Li}}$ . The strong PL near 450 nm, excited through the 375 nm band and becoming much more intense after vacuum annealing was associated with anion vacancies,  $\text{V}_{\text{S}}$ . Photoinduced absorption in the  $<850 \text{ nm}$  spectral range was observed after UV illumination of LGS. The PIA effect is reversible and the initial transparency can be restored by heating or illumination at longer wavelengths.

## ACKNOWLEDGMENTS

We acknowledge support from DLR (International Bureau of BMBF) under project RUS 08/013 and from the European Community's Seventh Framework Programme FP7/2007-2011 under grant agreement n° 224042.

## REFERENCES

- <sup>1</sup> A. A. Kaminskii, "Laser crystals and ceramics: recent advances," *Laser & Photon. Rev.* **1**, 93-177 (2007).
- <sup>2</sup> V. Petrov, F. Noack, I. Tunchev, P. Schunemann, and K. Zawilski, "The nonlinear coefficient  $d_{36}$  of  $\text{CdSiP}_2$ ," *Proc. SPIE* **7197**, 7197-21/1-8 (2009).
- <sup>3</sup> L. Isaenko, A. Yelisseyev, S. Lobanov, P. Krinitsin, V. Petrov, and J.-J. Zondy, "Ternary chalcogenides  $\text{LiBC}_2$  (B=In, Ga; C=S, Se, Te) for mid-IR nonlinear optics", *J. Non-Cryst. Sol.* **352**, 2439-2443 (2006).
- <sup>4</sup> J.-J. Zondy, V. Petrov, A. Yelisseyev, L. Isaenko, and S. Lobanov, "Orthorhombic crystals of lithium thioindate and selenoindate for nonlinear optics in the mid-IR," In: *Mid-Infrared Coherent Sources and Applications*, ed. by M. Ebrahim-Zadeh and I. Sorokina, *NATO Science for Peace and Security Series - B: Physics and Biophysics*, Springer (2008), pp. 67-104.
- <sup>5</sup> V. Petrov, A. Yelisseyev, L. Isaenko, S. Lobanov, A. Titov, and J.-J. Zondy, "Second harmonic generation and optical parametric amplification in the mid-IR with orthorhombic biaxial crystals  $\text{LiGaS}_2$  and  $\text{LiGaSe}_2$ ," *Appl. Phys. B* **78**, 543-546 (2004).
- <sup>6</sup> L. Isaenko, I. Vasilyeva, A. Yelisseyev, S. Lobanov, V. Malakhov, L. Dovlidova, J.-J. Zondy, and I. Kavun, "Growth and characterization of  $\text{LiInS}_2$  single crystals," *J. Cryst. Growth* **218**, 313-322 (2000).
- <sup>7</sup> L. Isaenko, A. Yelisseyev, S. Lobanov, A. Titov, V. Petrov, J.-J. Zondy, P. Krinitsin, A. Merkulov, V. Vedenyapin, and J. Smirnova, "Growth and properties of  $\text{LiGaX}_2$  (X=S, Se, Te) single crystals for nonlinear optical applications in the mid-IR", *Cryst. Res. Technol.* **38**, 379-387 (2003).

- <sup>8</sup> V. L. Bonch-Bruевич and V. B. Glasko, "The theory of electronic states connected with dislocations. 1. Linear dislocations," *Sov. Phys. Solid State* **3**, 26-33 (1961) [transl. from *Fiz. Tverd. Tela* **3**, 36-46 (1961)].
- <sup>9</sup> V. F. Kokorina, *Glasses for infrared optics*, CRC Press, Boca Raton, Florida, USA, 1996, p. 236.
- <sup>10</sup> M. V. Kurik, "Urbach rule," *Phys Stat. Sol. (a)* **8**, 9-45 (1971).
- <sup>11</sup> L. Isaenko, I. Vasilyeva, A. Merkulov, A. Yelisseyev, and S. Lobanov, "Growth of new nonlinear crystals LiMX<sub>2</sub> (M=Al, In, Ga; X=S, Se, Te) for the mid-IR optics," *J. Cryst. Growth* **275**, 217-223 (2005).
- <sup>12</sup> I. V. Bodnar and M. V. Yakushev, "Low-temperature photoluminescence of AgGaSe<sub>2</sub> single crystals," *Techn. Phys.* **49**, 335-337 (2004) [transl. from *Zh. Tekhn. Fiz.* **74**, 55-57 (2004)].
- <sup>13</sup> H. Mabuchi, E. S. Polzik, and H. J. Kimble, "Blue-light-induced IR absorption in KNbO<sub>3</sub>," *J. Opt. Soc. Am. B* **11**, 2023-2029 (1994).